

Theory of incommensurate magnetic correlations across the insulator-superconductor transition in underdoped $\text{La}_{2-x}\text{Sr}_x\text{CuO}_4$

Oleg P. Sushkov^{1,*} and Valeri N. Kotov^{2,†}

¹*School of Physics, University of New South Wales, Sydney 2052, Australia*

²*Institute of Theoretical Physics, Swiss Federal Institute of Technology (EPFL),*

CH-1015 Lausanne, Switzerland

(Dated: November 20, 2018)

The main feature in the elastic neutron scattering of $\text{La}_{2-x}\text{Sr}_x\text{CuO}_4$ is the existence of incommensurate peaks with positions that jump from 45° to 0° at 5% doping. We show that the spiral state of the $t - t' - t'' - J$ model with realistic parameters describes this data perfectly. We explain why in the insulator the peak is at 45° while it switches to 0° precisely at the insulator-metal transition. The calculated positions of the peaks are in agreement with the data in both phases.

PACS numbers: 74.72.Dn, 75.10.Jm, 75.30.Fv, 75.50.Ee

Introduction. The phase diagram of $\text{La}_{2-x}\text{Sr}_x\text{CuO}_4$ (LSCO) shows that the magnetic state changes dramatically with Sr doping. The parent compound La_2CuO_4 exhibits three-dimensional long-range antiferromagnetic (AF) order below 325K [1]. The Néel order disappears at Sr concentration $x \approx 0.02$, however two-dimensional (2D) short-range AF correlations exist at any doping [2] (see also Ref. [3] for a review). At $x \leq 0.055$ the system exhibits only hopping conductivity and behaves like an Anderson insulator, while the usual dc conductivity as well as superconductivity appear at $x > 0.055$ [2, 3].

Static magnetic ordering at very low temperatures has been observed both for $x < 0.055$ and $x > 0.055$. The elastic neutron scattering peak is close to the AF position $\mathbf{Q}_0 = (\pi, \pi)$, but is shifted from this position by $\delta\mathbf{Q}$: $\mathbf{Q} = \mathbf{Q}_0 + \delta\mathbf{Q}$. We set the lattice spacing $a = 1$. This shift indicates a one-dimensional incommensurate spin modulation. The dependence of the shift on doping has been studied in the superconducting phase [4], as well as in the insulating phase [5, 6, 7]. These studies have revealed the following remarkably simple dependence of the elastic peak shift on doping x (see Fig. 7 in [7]):

$$\begin{aligned} 0.055 < x < 0.12 : \quad & \delta\mathbf{Q} \approx 2x(\pm\pi, 0) \text{ or } \delta\mathbf{Q} \approx 2x(0, \pm\pi) , \\ 0.02 < x < 0.055 : \quad & \delta\mathbf{Q} \approx \sqrt{2}x(\pm\pi, \mp\pi) . \end{aligned} \quad (1)$$

Thus the 1D incommensurate spin modulation is proportional to doping and the direction jumps from 45° to 0° exactly at the point of the insulator-metal transition.

One of the early proposals made by Shraiman and Siggia in Ref. [8], and later explored in the context of the Hubbard and the t - J models [9, 10, 11, 12, 13, 14, 15], was that for small doping the collinear Néel order gives way to a non-collinear spiral state. There is a gain in energy since the holes can hop easier in a spiral background. However the issue of stability of the spiral state remained rather controversial. Using chiral perturbation theory [16] we have recently revisited the problem of stability of the spiral state in the extended $t - t' - t'' - J$ model [15], and have found that the uniform (1,0) spiral

state is stable (at low doping) above some critical values of t', t'' . The stability is due to quantum fluctuations (order from disorder effect). Even more importantly, superconductivity coexists with the spiral order. The starting point of the approach [15] is the ground state of the Heisenberg model which incorporates all spin quantum fluctuations. The chiral perturbation theory allows a regular calculation of all physical quantities in the leading order approximation in powers of doping x . Subleading powers of x depend on the short-range dynamics and hence cannot be calculated without uncontrolled approximations. Therefore the approach is parametrically well justified in the limit $x \ll 1$. The phase diagram of the $t - t' - t'' - J$ model obtained in Refs. [15] is presented in Fig. 1. From the Raman data [17] $J \approx 125\text{meV}$ and we set $t/J = 3.1$, following the calculations of Andersen *et al* [18]. The values $t' \approx -0.5J$, $t'' \approx 0.3J$ for LSCO and $t' \approx -0.8J$, $t'' \approx 0.6J$ for YBCO are taken from the same calculation. From now on we measure all energies in units of J ($J = 1$). The matrix elements t' and t'' are small compared to t , but nevertheless are crucially important for the stability because they influence substantially the hole dispersion. The pitch of the uniform superconducting spiral state is [15]

$$\delta\mathbf{Q} = \frac{Zt}{\rho_s} x (1, 0) \approx 5.8 x (1, 0) , \quad (2)$$

where $\rho_s \approx 0.18$ is the spin stiffness of the Heisenberg model and $Z \approx 0.34$ is the quasiparticle residue. The residue depends weakly on t' and t'' , and 0.34 is the value for LSCO [15]. Notice that Eq. (2) is in very good agreement with the data (1) in the metallic phase, $x > 0.055$. However different analysis is needed to explain the data (1) in the insulating region, $x < 0.055$.

In what follows we will consider mostly the insulating phase. The possibility of spiral ordering in the insulator has been stressed recently by Hasselmann *et al* [19]. However, the dynamical origin of the spiral, the pitch of the spiral as well as the “jump” of the spiral direction at the insulator-metal transition still remain unex-

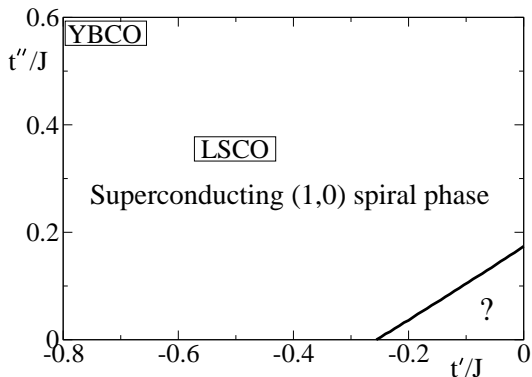


FIG. 1: The phase diagram of the $t-t'-t''-J$ model at $t/J = 3.1$ and small **uniform** doping [15]. Points corresponding to LSCO and YBCO are shown. The line separates the stable spiral phase and the unstable region (labeled “?”).

plained. It is the purpose of the present work to explain all these phenomena. In essence our idea is the following. The spiral (1,0)-state of the conductor has lower energy than that of the (1,1)-state only due to the presence of the Fermi motion energy [15]. On the other hand without the Fermi motion contribution the (1,1)-energy is lower than the (1,0)-energy. In the region $x < 0.055$ each hole is localized near its Sr ion, hence there is no Pauli blocking (Fermi energy) and the system immediately crosses over to the (1,1) spiral state. Following this line of reasoning we will demonstrate below that the whole variety of experimental data in the insulator and across the insulator-metal boundary can be consistently explained. In the insulator the ground state is strongly non-uniform, with the holes trapped in the vicinity of the randomly distributed Sr ions, as confirmed by the variable range hopping (VRH) behavior of the dc conductivity for $x < 0.055$ [3, 20]. Due to the presence of the Coulomb potential (see below) and disorder, it seems likely that the transition to the metallic (uniform) phase at $x = 0.055$ is of the density-driven percolation type. Thus we adopt this point of view although the exact nature of the transition is not crucially important for our analysis.

Coulomb trapping of holes. Let us consider first a single Sr ion with a single hole in an AF background. The hole is trapped near Sr by the Coulomb potential $e^2/(\epsilon_e \sqrt{r^2 + d^2}) \approx e^2/(\epsilon_e r)$ where d is the distance from the CuO_2 plane to the Sr ion and ϵ_e is the effective dielectric constant. For zero doping $\epsilon_e \sim 30$ and it increases with doping, as discussed in [3]. In momentum space the hole is localized near one of the points $\mathbf{k}_0 = (\pm\pi/2, \pm\pi/2)$, which are the centers of the four faces of the magnetic Brillouin zone (MBZ). In the vicinity of these points the dispersion is quadratic: $\epsilon_{\mathbf{k}} \approx \frac{\beta_1}{2} k_1^2 + \frac{\beta_2}{2} k_2^2$, where \mathbf{k} is defined with respect to \mathbf{k}_0 , and k_1 is perpendicular to the face of the MBZ, while k_2 is parallel to it. For values of t' and t'' corresponding to

LSCO we find that the dispersion is practically isotropic $\beta_1 \approx \beta_2 = \beta \approx 2.2$ [15]. Since the lattice spacing is about 3.85\AA this value corresponds to an effective mass of about two free electron masses, in agreement with the optical conductivity data [3]. The solution of the Schrödinger equation

$$(-\beta \nabla^2/2 - e^2/(\epsilon_e r)) \chi = \epsilon \chi \quad (3)$$

determines the ground state wave function and the ground state energy of the localized hole:

$$\chi(r) = \sqrt{2/\pi\kappa} e^{-\kappa r}, \quad \epsilon = -\beta\kappa^2/2 \quad (4)$$

where $\kappa = 2e^2/(\epsilon_e \beta)$. Using the hopping conductivity data at very low doping ($x = 0.002$) [21] we estimate the inverse size $\kappa \approx 0.4$. At higher doping (but still in the insulator) the value of κ might decrease slightly. Thus throughout the insulating phase κ is small and this justifies the semiclassical approximation we use below. Note that the semiclassical approximation is used only with respect to the kinetic energy of the hole but not for the spin (we do not use the $1/S$ expansion and account for all spin quantum fluctuations via the chiral perturbation theory [15]).

Spiral induced by a single trapped hole. Equations (3) and (4) assume a rigid antiferromagnetic background. However one can gain energy relaxing the background into the spiral state. In the spiral state there are still two sublattices, sublattice “up” and sublattice “down”, but the spin at every site of each sublattice is rotated by an angle θ_i with respect to the orientation at $r = \infty$

$$\begin{aligned} |i\rangle &= e^{i\theta(\mathbf{r}_i)\mathbf{m}\cdot\sigma/2} |\uparrow\rangle, \quad i \in \text{“up” sublattice}, \\ |j\rangle &= e^{i\theta(\mathbf{r}_j)\mathbf{m}\cdot\sigma/2} |\downarrow\rangle, \quad j \in \text{“down” sublattice}. \end{aligned} \quad (5)$$

Here $\mathbf{m} = (\cos \alpha, \sin \alpha, 0)$ with arbitrary α is the “director” of the spiral which is orthogonal to the magnetization plane. Note that directions in spin space are completely independent of directions in coordinate space. The wave function of the hole $\psi(\mathbf{r})$ has two components corresponding to up and down sublattices. The total energy is of the form [12, 15]

$$E = \int d^2r \left\{ \frac{\rho_s}{2} (\nabla\theta)^2 + \psi^\dagger(\mathbf{r}) \begin{pmatrix} -\beta\frac{\nabla^2}{2} - \frac{e^2}{\epsilon_e r} & \sqrt{2}Zte^{-i\alpha}(\mathbf{e}\cdot\nabla\theta) \\ \sqrt{2}Zte^{i\alpha}(\mathbf{e}\cdot\nabla\theta) & -\beta\frac{\nabla^2}{2} - \frac{e^2}{\epsilon_e r} \end{pmatrix} \psi(\mathbf{r}) \right\}, \quad (6)$$

where $\mathbf{e} = (\frac{1}{\sqrt{2}}, \pm\frac{1}{\sqrt{2}})$ is a unit vector orthogonal to a given face of the MBZ. Let us search for a solution in the form

$$\psi(\mathbf{r}) = \frac{1}{\sqrt{2}} \begin{pmatrix} 1 \\ -e^{i\alpha} \end{pmatrix} \chi(r) \quad (7)$$

where $\chi(r)$ is given by Eq. (4). Variation of the energy (6) with respect to θ leads to the following equation

$$\nabla^2\theta = \sqrt{2}\frac{Zt}{\rho_s}(\mathbf{e}\cdot\nabla)\chi^2(r). \quad (8)$$

The solution of (8) is

$$\theta = \frac{Zt}{\sqrt{2\pi\rho_s}} \frac{(\mathbf{e} \cdot \mathbf{r})}{r^2} [1 - e^{-2\kappa r} (1 + 2\kappa r)] . \quad (9)$$

Substitution of this solution together with (7) and (4) in Eq. (6) gives the following total energy

$$E = \left(\frac{\beta}{2} - \frac{Z^2 t^2}{4\pi\rho_s} \right) \kappa^2 - 2 \frac{e^2}{\epsilon_e} \kappa . \quad (10)$$

Minimizing this energy one finds $\kappa = \frac{2e^2}{\epsilon_e} / [\beta - Z^2 t^2 / (2\pi\rho_s)]$. However we do not use directly this expression since the effective dielectric constant ϵ_e is not known accurately enough. Instead we rely on estimates for κ which directly follow from the hopping conductivity as discussed after Eq. (4). As can be easily seen from Eqs. (5,9), at distances $r \ll 1/\kappa$ our solution describes a $(1, \pm 1)$ spiral, while in the opposite limit an effective dipole is formed (see discussion below). The solution is a variational one because we have used the ansatz (4). Even though one can easily derive an exact equation for χ which can be solved numerically, this is not necessary since for our purposes the details of the charge distribution are not important.

We emphasize that the Coulomb trapping of the hole is crucially important. Without such trapping the hole is delocalized and a single delocalized hole does not generate a static spiral. This is qualitatively different from the arguments of Ref. [22]. The solution (9) does not carry any topological numbers, and consequently, unlike the model used in Ref. [23], our solution is *not* a skyrmion. Other topological reasons for “self-trapping” of holes have also been given [24], however we pursue the Coulomb trapping picture since it unambiguously follows from the parametrically justified analysis of the t-J model.

The solution (5),(9) depends on the spiral “director” which is a purely classical variable and the energy is independent of it. It is unlikely that a finite system has an exactly degenerate ground state (spontaneous violation of symmetry). This means that higher orders in κ (κ^4 -corrections to the semiclassical solution) may give rise to a kinetic energy for the director \mathbf{m} and hence to quantum rotations of \mathbf{m} , lifting the degeneracy. Another quantum effect is tunneling from one pocket in momentum space to another. However, the quantum corrections are not important for understanding the properties of LSCO since at finite concentration of impurities the interaction between them is much more important than the quantum corrections to the semiclassical limit.

Effective dipole moment of the impurity and destruction of the Néel order at 2% doping. It is convenient to rewrite Eq. (9) using the notation of the non-linear σ -model. Far from the impurity core, $r \gg 1/\kappa$, the solution

reads

$$\delta \mathbf{n} = \overline{\mathbf{m}} \theta = \overline{\mathbf{m}} M \frac{(\mathbf{e} \cdot \mathbf{r})}{2\pi r^2} , \quad M = \frac{\sqrt{2} Z t}{\rho_s} \approx 8.2 \quad (11)$$

where $\mathbf{n} = \delta \mathbf{n} + \mathbf{n}_0$ is the unit vector of antiferromagnetism, $\mathbf{n}_0 = \mathbf{n}(r = \infty)$, $\overline{\mathbf{m}} = [\mathbf{n}_0 \times \mathbf{m}]$, and \mathbf{m} is the director of the impurity. Here M is the effective dipole moment of the impurity. Note that it is very large, $M \gg 1$.

The idea of destruction of the Néel order by randomly quenched dipoles was put forward by Glazman and Iosevich [25]. Detailed renormalization group calculations based on this picture have been performed by Cherepanov *et al* [26] and we use their results. In particular an analysis of the experimental data by Keimer *et al* [2] for the in-plane correlation length at $x < 0.02$ was performed in [26]. This analysis shows that in order to explain the data and hence the destruction of the Néel order at $x \approx 0.02$ one needs to have a value of M which satisfies the following condition [26]

$$A = \frac{M^2}{\mathcal{N}d} = 20(1 \pm 0.3) . \quad (12)$$

Here $d = 2$ is the dimensionality of the problem and \mathcal{N} is the dimensionality of the vector $\overline{\mathbf{m}}$. In our theory $\mathcal{N} = 2$ because $\overline{\mathbf{m}}$ is orthogonal to \mathbf{n}_0 . Hence we conclude from (12) that $M_{exp} = 8.9(1 \pm 0.15)$. This agrees well with the theoretical value (11).

Structure of the insulating (spin glass) region and transition into the metallic phase. Here we consider the range of doping $0.02 < x < 0.055$ where the insulating spin glass state is realized. Since elastic incommensurate neutron peaks have been observed in this regime [5, 6, 7], there are two characteristic length scales: $l_I \propto 1/x$, related to the incommensurability, and the magnetic correlation length $l_M > l_I$, related to the spin glass disorder (randomness) and reflected in the (inverse) width of the elastic neutron peaks.

It is clear that in order to minimize the dipole-dipole interaction energy at finite impurity concentration (and at zero temperature), the dipoles (11) will align in such a way that all vectors \mathbf{e} and $\overline{\mathbf{m}}$ are the same. Such an alignment is possible in spite of the random positions and generates an average spiral [19]. Certainly around each dipole there are deviations from the average described by (9). One can consider the average spiral as a self-consistent field created by all dipoles. To find the average pitch of the spiral let us consider a single dipole with field $\delta \mathbf{n}$ given by (11) in a background field $\mathbf{n}_b = \mathbf{n}_0 + \delta \mathbf{n}_b$ where

$$\delta \mathbf{n}_b = -\lambda \overline{\mathbf{m}}_b (\mathbf{e}_b \cdot \mathbf{r}) . \quad (13)$$

Here $\delta \mathbf{n}_b$ is the self-consistent field of the dipoles, $\mathbf{e}_b = (1/\sqrt{2}, \pm 1/\sqrt{2})$ is a unit vector orthogonal to the face of MBZ, and λ is a parameter. The interaction of the dipole with the background field is given by: $\frac{\rho_s}{2} \int (\nabla \delta \mathbf{n} + \nabla \delta \mathbf{n}_b)^2 d^2 r - \frac{\rho_s}{2} \int (\nabla \delta \mathbf{n})^2 d^2 r - \frac{\rho_s}{2} \int (\nabla \delta \mathbf{n}_b)^2 d^2 r$, which

simply amounts to $\rho_s \int (\nabla \delta \mathbf{n}) (\nabla \delta \mathbf{n}_b) d^2 r = -M \rho_s (\overline{\mathbf{m}} \cdot \overline{\mathbf{m}}_b) (\mathbf{e} \cdot \mathbf{e}_b)$. Clearly the interaction energy has a minimum at $\overline{\mathbf{m}} = \overline{\mathbf{m}}_b$ and $\mathbf{e} = \mathbf{e}_b$. The total energy at a finite concentration x consists of the energy of each particular impurity (10), the interaction energy, and the elastic energy of the background:

$$E_\lambda = Ex - \rho_s CM \lambda x + \frac{\rho_s}{2} \lambda^2. \quad (14)$$

In the interaction energy term we have introduced the finite-size correction constant C . Indeed, Eq. (11) is valid only at very large distances from the impurity. However at a finite distance the effective dipole moment is reduced, according to Eq. (9), by the amount $C = [1 - e^{-2\kappa r} (1 + 2\kappa r)]$. Substituting $r = 1/\sqrt{\pi x}$ and $\kappa \approx 0.4$, we find for $x = 0.03 - 0.05$ the value $C \approx 0.7$. Minimizing (14) with respect to λ we find $\lambda = CMx$. Hence the average pitch is

$$\delta \mathbf{Q} = \lambda \mathbf{e}_b = C \frac{Zt}{\rho_s} x (1, \pm 1). \quad (15)$$

This expression determines the incommensurate shift of the neutron peak and agrees well with the experimental data (1) since $CZt/\rho_s \approx 4.1$.

The last question we want to discuss is the microscopic origin of the correlation length l_M . First we notice that without randomness we would automatically have $l_M = \infty$, whereas experimentally this quantity is about $l_M \approx 25 - 40 \text{ \AA}$ [7]. It has been suggested in Ref. [19] that topological defects related to the random positions of impurities can destroy the long-range spiral order. This is a possible scenario, however we suggest a different mechanism. In our opinion even randomly distributed dipoles (11) would create a true long-range spiral order, similarly to a 2D ferroelectric. However, our main observation is that the situation is *not* fully described by the point-like dipoles. Each impurity has a *finite size core* (see Eq. (9)) with diameter $1/\kappa \sim 3 - 5$ lattice spacings (depending on doping). Therefore, given a random distribution of positions, there is always a finite probability of impurity overlap. As soon as the impurities overlap, a two-hole “molecule” is formed and the situation changes dramatically. In the “molecule” the Pauli blocking starts to play a role and in order to minimize the energy the holes prefer to occupy different pockets in momentum space. If two pockets are occupied the (1,0) spiral has lower energy, and this is exactly what happens in the conducting phase [15]. Hence such a “molecule” has a local spiral along (1,0) or (0,1) direction. This spiral frustrates the (1,1) background and there is always a finite concentration of such frustrating dipoles. Hence the “molecule” dipoles destroy the (1,1) background similarly to the way the “atomic” (single) dipoles destroy the Néel background at $x < 0.02$. One can consider these “molecules” as a precursor to the transition to the conductor where the (1,0) spiral is realized. According to

this picture the spin-glass correlation length l_M is large (but always finite) at very small x and it should decrease dramatically towards the percolation point $x \approx 0.055$ where the “molecular” configurations are becoming more important. This is exactly what is observed in experiment, as seen in Fig. 6 of Ref. [7]. In the superconducting phase the magnetic correlation length should increase very rapidly, since theoretically it is infinity in the fully uniform, metallic phase [15]. Indeed, experimentally the correlation length quickly approaches the uniform limit [7] (it is $> 200 \text{ \AA}$, $x = 0.12$).

In conclusion, we have developed a description of the magnetic properties of underdoped $\text{La}_{2-x}\text{Sr}_x\text{CuO}_4$, based on the extended $t-J$ model. The theory describes the incommensurate elastic neutron scattering above and below the metal-insulator transition at $x = 0.055$. In particular it explains why the incommensurate peak position rotates by 45° exactly at the insulator-metal transition. The theory does not contain any fitting parameters, and the positions of the neutron peaks both in the conducting (2) and in the insulating (15) phases, as well as the critical concentration for destruction of the Néel order, follow from the calculated parameters of the extended $t-J$ model. We also note that in $\text{La}_{2-x}\text{Sr}_x\text{CuO}_4$ static charge modulation (stripes) has not been directly observed, suggesting that it is very weak or not present at all. We thus believe that a theory based on spiral magnetic correlations and no charge order is fully sufficient to describe the phenomena in this material.

We are grateful to J. Haase, A. H. Castro Neto, G. V. M. Williams, O. K. Andersen, M. Ain, P. A. Lee, and Y. S. Lee for important discussions and comments. The support of the Swiss National Fund is acknowledged (V NK).

* Electronic address: sushkov@phys.unsw.edu.au

† Electronic address: valeri.kotov@epfl.ch

- [1] B. Keimer *et al.*, Phys. Rev. B **45**, 7430 (1992).
- [2] B. Keimer *et al.*, Phys. Rev. B **46**, 14034 (1992).
- [3] M. A. Kastner, R. J. Birgeneau, G. Shirane, and Y. Endoh, Rev. Mod. Phys., **70**, 897 (1998).
- [4] K. Yamada *et al.*, Phys. Rev. B **57**, 6165 (1998).
- [5] S. Wakimoto *et al.*, Phys. Rev. B **60**, R769 (1999).
- [6] M. Matsuda *et al.*, Phys. Rev. B **62**, 9148 (2000).
- [7] M. Fujita *et al.*, Phys. Rev. B **65**, 064505 (2002).
- [8] B. I. Shraiman and E. D. Siggia, Phys. Rev. Lett. **62**, 1564 (1989).
- [9] C. L. Kane *et al.*, Phys. Rev. B **41**, 2653 (1990).
- [10] A. Auerbach and B. E. Larson, Phys. Rev. B **43**, 7800 (1991).
- [11] A. Singh, Z. Tesanovic, and J. H. Kim, Phys. Rev. B **44**, 7757 (1991).
- [12] J. Igarashi and P. Fulde, Phys. Rev. B **45**, 10419 (1992).
- [13] A. P. Kampf, Phys. Rep. **249**, 219 (1994) and references therein.
- [14] A. V. Chubukov and K. A. Musaelian, Phys. Rev. B **51**,

- 12605 (1995).
- [15] O. P. Sushkov and V. N. Kotov, Phys. Rev. B **70**, 024503 (2004); V. N. Kotov and O. P. Sushkov, Phys. Rev. B **70**, 195105 (2004).
- [16] S. Weinberg, Phys. Rev. Lett. **17**, 616 (1966); Phys. Rev. **166**, 1586 (1968); S. L. Adler, Phys. Rev. **137**, B1022 (1965). See also: F. Hasenfratz and F. Niedermayer, Z. Phys. B **92**, 91 (1993) and references therein.
- [17] Y. Tokura *et al.*, Phys. Rev. B **41**, 11657 (1990).
- [18] O. K. Andersen, A. I. Liechtenstein, O. Jepsen, and F. Paulsen, J. Phys. Chem. Solids **56**, 1573 (1995); E. Pavarini *et al.*, Phys. Rev. Lett. **87**, 047003 (2001).
- [19] N. Hasselmann, A. H. Castro Neto, and C. Morais Smith, Phys. Rev. B **69**, 014424 (2004).
- [20] E. Lai and R. J. Gooding, Phys. Rev. B **57**, 1498 (1998).
- [21] C. Y. Chen *et al.*, Phys. Rev. B **51**, 3671 (1995).
- [22] B. I. Shraiman and E. D. Siggia, Phys. Rev. Lett. **61**, 467 (1988); V. Elser, D. A. Huse, B. I. Shraiman, and E. D. Siggia, Phys. Rev. B **41**, 6715 (1990); B. I. Shraiman, and E. D. Siggia, Phys. Rev. B **42**, 2485 (1990).
- [23] R. J. Gooding, Phys. Rev. Lett. **66**, 2266 (1991).
- [24] S. P. Kou and Z. Y. Weng, Phys. Rev. B **67**, 115103 (2003); S. P. Kou and Z. Y. Weng, cond-mat/0402327.
- [25] L. I. Glazman and A. S. Ioselevich, Z. Phys. B **80**, 133 (1990).
- [26] V. Cherepanov, I. Ya. Korenblit, A. Aharony, and O. Entin-Wohlman, Eur. Phys. J. B **8**, 511 (1999).